Journal of Hydroscience and Hydraulic Engineering
Vol. 17, No.2 November, 1999, 1-9

APPLICABILITY OF A GEOMORPHOLOGY-BASED HYDROLOGICAL MODEL IN LARGE CATCHMENTS

By

Dawen Yang, Srikantha Herath and Katumi Musiake

Institute of Industrial Science, University of Tokyo, 7-22-1 Roppongi, Minato-ku, Tokyo, 106-8558, Japan

SYNOPSIS

The grid-based distributed hydrological models are powerful tools for hydrological modeling due to the representation of the spatial variability and the physically based process descriptions. However, because of the large computational demands this kind of models is not suitable for long term simulations in large catchments. Here, an alternative distributed hydrological model is proposed, which is based on the catchment geomorphology area function and width function. In this model, the catchment is discretized into a number of flow intervals along the flow direction. Each flow interval is represented as a series of hillslope elements. A physically-based hillslope response model and the kinematic wave model are used to simulate the runoff generation and flow routing. The applicability of the model for the simulation of multiple catchments is discussed in the paper.

INTRODUCTION

The distributed hydrological modeling is necessary when the spatial distribution of hydrologic variables are important. In general, for distributed hydrologic modeling, the catchments are discretized into a number of small grids. However, large computational demands and model complexities are a deterrent to the use of distributed hydrologic models in very large catchments, such as for coupling with regional atmospheric models. Therefore a new type of hydrological model is necessary for large catchments. The catchment geomorphologic area function and width function used by Yang et al. (1) provides a possibility to quantitatively describe the catchment heterogeneity. The area function shows the aggregating pattern of the catchment. Naden (2) described the rainfall and soil properties in a hydrological model coupled with width function. Yang et al. (3) used area function to describe the rainfall distribution for modeling flood by coupling with the tank model. Here we present a method, which employs the geomorphologic area function and width function to reduce the catchment lateral dimension from two to one. The methodology makes it possible to reduce the 2-dimensional spatial data to 1-dimensional distribution functions of characteristics with respect to flow distance from the catchment outlet, which improve the hydrological modeling efficiency while retaining the spatial heterogeneity information. This methodology was used for simulating floods (4). The main objective of this paper is to investigate the applicability of the geomorphology-based hydrological model in large catchments.

MODEL DESCRIPTION

(1) Catchment Discretization

When the river network is generated using a flow accumulation method, the flow direction of each cell is determined according to the steepest descent direction. Following the flow direction, the flow distance of each cell from the catchment outlet can be calculated. The area function can be

uniquely derived from this method. Considering any flow interval Δx at distance x, the catchment area accumulated in this interval is given by the area function. For hydrological modeling, the catchment is divided into a number of flow intervals (Figure 1). Each flow interval is represented using a number of hillslope elements. The number of hillslope elements depends on the number of streams within the same flow interval. The spatially distributed parameters of the catchment, such as rainfall, elevation and hillslope angle, are averaged for each flow interval. Similar to area function, the spatial distributed catchment parameters are given by distribution functions.

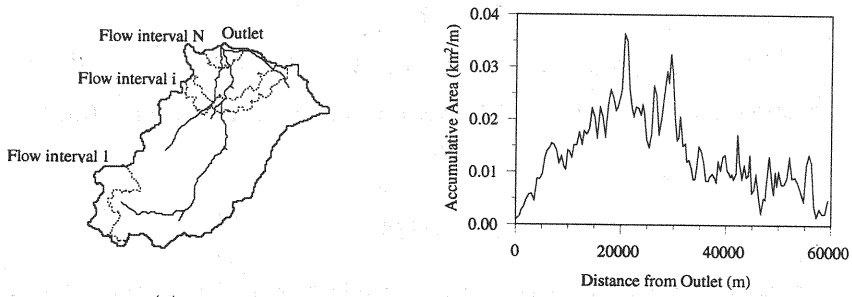

Figure 1 (a) Flow Interval and (b) the Area Function

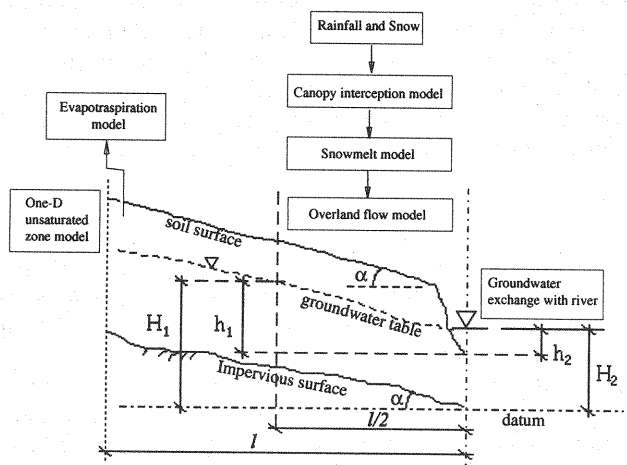

Figure 2 Hillslope Model

(2) Hillslope Response Model

The hillslope element is assumed as a rectangular inclined plane with width of flow interval length Δx, length of l and angle α. The bed rock slope is assumed to be parallel to the surface. The hillslopes are located in both sides of the river symmetrically (Figure 2). The hydrological processes on hillslope include interception, evapotranspiration, infiltration, overland flow, unsaturated soil water and groundwater flow. In the hillslope model, the vertical plane is divided into several layers, including canopy, soil surface, a number of soil zones (parallel to the surface) and shallow groundwater layer. For each layer, simple storage-based models are used. The macro-pores in the top soil is represented using an anisotropy ratio, defined as

$$a_r = K_{sp} / K_{sn} > 1 \qquad (1)$$

where a_r = the anisotropy ratio, K_{sp} and K_{sn} = the saturated hydraulic conductivity (mm h^{-1}) in the directions normal and parallel to the slope respectively. The exponential assumption is adopted here

for representing the decrease of hydraulic conductivity with depth, given as

$$K_s(z) = K_0 \exp(-f z) \tag{2}$$

where $K_s(z)$ = the saturated hydraulic conductivity at a depth z (mm h^{-1}), z = the distance taken positive in the downward direction normal to the surface (m), K_0 = the saturated conductivity at the surface (mm h^{-1}), f = constant parameter (m^{-1}).

a) Interception and Evapotranspiration

The interception capacity depends on the vegetation coverage and the leaf-area-index. Actual interception is determined by the precipitation amount and the deficit of the canopy water storage. Interception capacity is given by

$$S_{C0}(t) = I_0 K_v \frac{LAI(t)}{LAI_0} \tag{3}$$

The deficit of canopy water storage is

$$S_{Cd}(t) = S_{C0} - S_c(t) \tag{4}$$

where S_{C0} = the interception capacity (mm); I_0 = the maximum interception ability of the vegetation in a year (mm); K_v = the vegetation coverage; LAI = the leaf-area-index at time t; LAI_0 = the maximum leaf-area-index of the vegetation in a year; $S_{Cd}(t)$ = the deficit of canopy water storage (mm); $S_c(t)$ = the canopy water storage at time t (mm). Considering the uniform intensity rainfall $r(t)$ in a time interval $[t, t+\Delta t]$, the actual interception is determined as

$$Actual\ \ Interception = \begin{cases} r(t)\Delta t; & r(t)\Delta t \le S_{Cd}(t) \\ S_{Cd}(t); & r(t)\Delta t > S_{Cd}(t) \end{cases} \tag{5}$$

The potential evaporation is estimated using a radiation-based method according to the available data. Actual evapotranspiration is calculated as evaporation from canopy water storage, transpiration from a root zone, evaporation from surface storage and evaporation from the soil surface. The evaporation from soil surface is estimated as a function of average soil moisture content in the first zone. The evapotranspiration is assumed take place only during the daytime 12 hours and no rainfall. The daily potential evaporation is divided by 12 hours to convert it to hourly potential evaporation. Actual evaporation rate from canopy in a time interval $[t, t+\Delta t]$ is given by

$$E_{canopy}(t) = \begin{cases} K_v K_c E_p; & S_c(t) \ge K_v K_c E_p \Delta t \\ Sc(t)/\Delta t; & S_c(t) < K_v K_c E_p \Delta t \end{cases} \tag{6}$$

where E_{canopy} = the actual evaporation rate from canopy storage (mm h^{-1}); E_p = the potential evaporation rate (mm h^{-1}); Δt = the time interval (h); K_c = crop coefficient. The vegetation transpiration rate from each soil zone in a time interval $[t, t+\Delta t]$ is written as

$$E_{tr}(t) = \left[K_v K_c K_p\right] f_1(z)\, f_2(\theta) \frac{LAI(t)}{LAI_0} \tag{7}$$

where $E_{tri}(t,i)$ = the transpiration rate (mm h^{-1}) from zone i at time t; f_1 = the root distribution function; $f_2(\theta)$ = soil moisture function; θ is the soil moisture content. The actual evaporation rate from soil

water storage in time interval [t, $t+\Delta t$] is given by

$$E_{surface}(t)=\begin{cases}E_p(1-K_v); & S_s(t)\geq E_p(1-K_v)\Delta t\\ S_s(t)/\Delta t; & S_s(t)<E_p(1-K_v)\Delta t\end{cases} \quad (8)$$

where $E_{surface}$ = the evaporation rate from surface water (mm h^{-1}); $S_s(t)$ = the surface water storage at time t (mm). The evaporation rate from the soil surface in time interval [t, $t+\Delta t$] is given by

$$E_s(t)=\{E_p(1-K_v)-E_{surface}(t)\}f_2(\theta) \quad (9)$$

where $E_s(t)$ = the evaporation rate from soil surface (mm h^{-1}).

b) Surface Runoff and Infiltration

The mass balance for the surface storage in the time interval [t, $t+\Delta t$] is given by

$$\Delta S_s(t+\Delta t)/\Delta t = P_n(t)+M_s(t)-q_s(t)-f_{in}(t)-E_{surface}(t) \quad (10)$$

where $\Delta S_s(t+\Delta t)$ = the change of surface water storage at time t during a time duration Δt (mm); $P_n(t)$ = the net rainfall intensity at time t (mm h^{-1}); $f_{in}(t)$ = the infiltration rate at time t (mm h^{-1}); $q_s(t)$ = the surface runoff (mm h^{-1}). The infiltration rate $f_{in}(t)$ is given by

$$f_{in}(t)=\begin{cases}P_n(t), & P_n(t)<K_0\\ K_0, & P_n(t)\geq K_0\end{cases} \quad (11)$$

where K_0 = the saturated hydraulic conductivity of the top soil (mm h^{-1}). The surface runoff $q_s(t)$ is calculated by

$$q_s(t)\Delta t=\begin{cases}S(t)-S_{\max}, & S(t)>S_{\max}\\ 0, & S(t)\leq S_{\max}\end{cases} \quad (12)$$

in which $S(t)$ = the surface water storage at time t (mm); S_{max} = the maximum surface storage (mm).

c) Unsaturated Zone

The top unsaturated soil is divided into multiple layers, the mass balance for layer i is given by

$$\Delta S_{sub_i}(t+\Delta t)/\Delta t = f_{i-1}(t)-f_i(t)-E_{tr_i}(t)-E_{s_i}(t) \quad (13)$$

where ΔS_{subi} = the change of water storage in layer i at time t during time interval Δt (mm); $f_i(t)$ = the recharge rate (mm h^{-1}) from layer i to layer $i+1$; $f_0(t)=f_{in}(t)$. The recharge rate $f_i(t)$ $(i>0)$ is given by

$$f_i(t)=\begin{cases}K(\theta_i)\dfrac{\partial(z+\psi)}{\partial z}\approx K(\theta_i); & \theta_i>\theta_f \text{ or } \theta_{i+1}\leq\theta_i\\ 0; & \theta_i\leq\theta_f \text{ and } \theta_{i+1}>\theta_i, z_{i+1}>z_i\end{cases} \quad (14)$$

in which θ_i = the soil moisture content in layer i; θ_f = the soil moisture content at field capacity; $K(\theta_i)$ = the hydraulic conductivity(mm h^{-1}).

d) Saturated Zone and Exchange with River

The basic equations used for the saturated zone are the equation of mass balance and Darcy's law. The equation of mass balance is give by

$$\Delta S_G(t+\Delta t)/\Delta t = rech(t) - L(t) - q_G(t)\frac{1000}{A_h} \tag{15}$$

where $\Delta S_G(t+\Delta t)$ = the change of groundwater storage (unconfined aquifer) (mm); $rech(t)$ = the recharge rate from a upper unsaturated zone (mm h^{-1}); $L(t)$ = the leakage to deep aquifer (mm h^{-1}); A_h = the plane area of a hillslope element (m^2 m^{-1}); $q_G(t)$ = the discharge to the river per unit width (m^3 h^{-1} m^{-1}), calculated as

$$q_G(t) = K_G \frac{H_1 - H_2}{l/2}\frac{h_1 + h_2}{2} \tag{16}$$

where K_G = the hydraulic conductivity of a unconfined aquifer; H_1, H_2, h_1 and h_2 are shown in Figure 2.

(3) Flow Routing

The kinematic wave model given by the continuity and momentum equations is used for flow routing and solved using explicit finite difference method.

$$\frac{\partial Q}{\partial x} + \frac{\partial A}{\partial x} = q_L\ ; \qquad q_L = q_S + q_G \tag{17}$$

The momentum equation is given by Manning's equation

$$Q = \frac{S_0^{1/2}}{n\ p^{2/3}} A^{5/3} \tag{18}$$

where x = the distance along the longitudinal axis of the river (m); t = the time (s); A = the cross-sectional area (m^2); Q = the discharge at x (m^3 s^{-1}); q_L = the lateral inflow (m^3 s^{-1} m^{-1}); S_0 = the river bed slope; n = Manning's roughness; p = the wetting perimeter (m).

INVESTIGATION OF MODEL PERFORMANCE

(1) Study Area

The Karasu River, which is located in the north of Tokyo, is selected for this study (Figure 3). The total catchment area is 1220.8 km^2 above the discharge-gauge D and 80% of the area is mountainous. It contains two main sub-catchments with areas of 536.3 km^2 (up to D-1) and 555.2 km^2 (up to D-2). There are 6 rain gauges within or near the catchment. Three-year data sets (1992–1994) of daily discharge and hourly rainfall are available. The daily temperature and sunshine duration data at two gauges are used to estimate the potential evaporation. The spatial distributions of rainfall and potential evaporation are given by Thiessen Polygons. The first year is used to initialize the initial condition by repeating the simulation twice and calibrate the model parameters. The calibrated parameters are the saturated hydraulic conductivity of the surface soil (with a value of 80.0 mm h^{-1}) and the hydraulic conductivity of groundwater (with values of 5.0 mm h^{-1} for sub-catchment D-1 and 1.0 mm h^{-1} for D-2). The anisotropy ratio in Eq. 2 is 5.0.

(2) Modeling Considerations

There are two basic considerations investigating the model performance: (a) Effect of flow interval length and (b) Effect of sub-catchment size. The simulations are carried out first, as a system with independent sub-catchments linked by the river network, and then, treating the whole area as a single catchment. A single land cover (forest) and a single soil type (Kanto loam) are used for the whole catchment in the analysis. Figure 4 shows the flow distance contours for the whole area treated as a single catchment. Figure 5 gives the flow distance contours for each sub-catchment from outlet of each catchment. The catchment spatial variations (only hillslope length and slope gradient are considered here) are averaged over the whole catchment in each flow interval in the case of the single whole catchment, but treated in each sub-catchment independently in the case of the sub-catchments system.

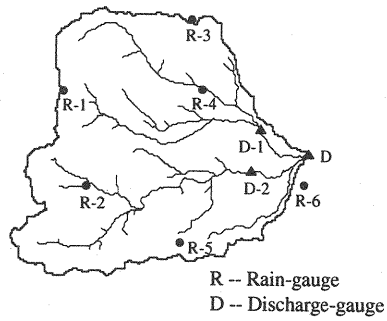

Figure 3 The Karasu River Catchment

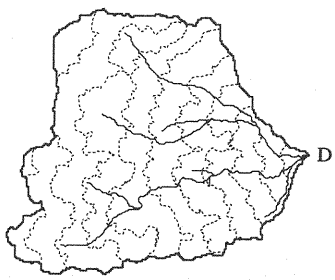

Figure4 Flow Distance Contours for the Whole Catchment

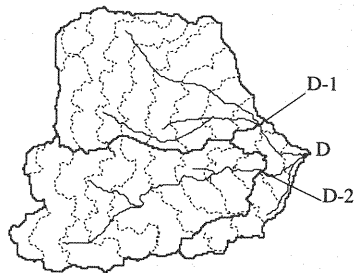

Figure 5 Flow Distance Contours for Each Sub-catchment

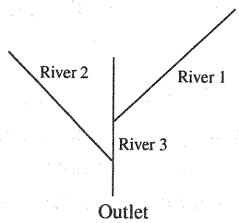

Figure 6 Simplified River Network

(3) Effect of Flow Interval Length

The whole catchment is divided into three sub-catchments: sub-catchment 1 (up to D-1), sub-catchment 2 (up to D-2) and sub-catchment 3 (the residual part). The hillslope responses of each sub-catchment are simulated independently. So that the river network of each sub-catchment is simplified using the main channels of each sub-catchment, a simplified river network is derived (Figure 6). The

flow intervals are determined automatically according to the main channel segments, and flow interval lengths are made to be less than 600 m or 300 m for two simulations. Figures 7 and 8 show the comparisons of simulated daily hydrographs with the observed ones at discharge-gauges D-1 and D-2 respectively for the case of a flow interval length less than 600 m. Table 1 shows the simulation error and CPU time (Dec-Alpha 433 MHz computer) for the two simulations for a period of two years. The simulation error is calculated in the simulation period (1993-1994) as

$$error = \frac{\Sigma\sqrt{(Q_o - Q_s)^2}}{N\overline{Q_o}} \tag{19}$$

where Q_o = the observed discharge; Q_s = the simulated discharge; $\overline{Q_o}$ = the mean value of the observed discharge; N = the total number of the discharge data in the simulation period.

Table 1 Effect of Flow Interval Length

Flow interval	Less than 600 m		Less than 300 m	
Sub-catchment	D-1	D-2	D-1	D-2
Error in Eq. 19 (%)	7.383	2.826	7.359	2.821
Computation time (s)	110		144	

The result shows that there is no significant difference between the two simulation results. But using of 600 m flow interval length saves 1/3 of the computation time. This is useful for applications in large catchments.

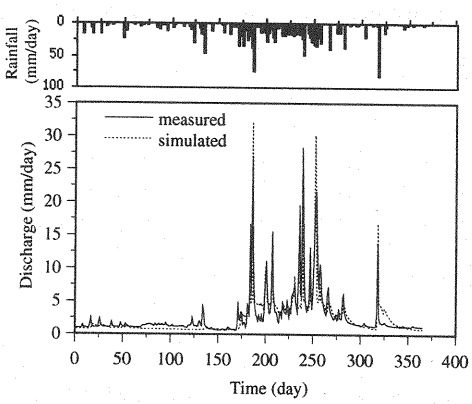

Figure 7 Hydrograph at D-1 for the Case of Flow Interval Length Less than 600m in 1993

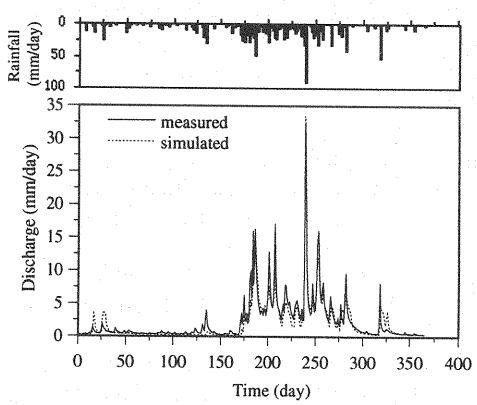

Figure 8 Hydrograph at D-2 for the Case of Flow Interval Length Less than 600m in 1993

(4) Effect of Sub-catchment Size

In the model, the hillslope parameters are averaged for each flow interval. If the catchment is too large, an error is introduced by the averaging procedure. In order to investigate the effects of averaging hillslope parameters, two simulations have been carried out. In the first case (single whole catchment), the hillslope parameters are averaged in whole catchment for each flow interval. In the second case (multiple sub-catchments: three sub-catchments), the hillslope parameters are averaged over each sub-catchment within individual flow intervals. For both cases, the flow interval lengths are less than 600 m. Figure 9 shows the comparisons of simulated daily hydrographs with the observed one at discharge-gauge D for the case of using the multiple catchments. Figure 10 gives the result for the case of using the single whole catchment. Table 2 shows the simulation errors and computation CPU time in the simulation period for both simulations.

Table 2 Effect of Sub-catchment Size

Simulation	Single whole catchment	Multiple sub-catchments
Error in Eq. 19 (%)	3.185	4.744
Computation time (s)	36	110

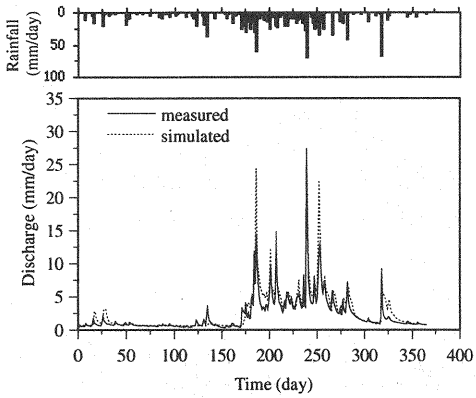

Figure 9 Hydrograph at D for the Case of Multiple Sub-catchments and Flow Interval Length Less than 600m in 1993

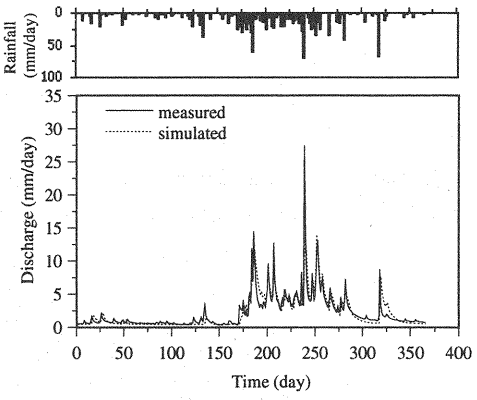

Figure 10 Hydrograph at D for the Case of Single Whole Catchment and Flow Interval Length Less than 600m in 1993

From the results, we can see that the simulation errors for the two cases are very close. But the computation time for the case of simulating single whole catchment is only 1/3 of simulating multiple catchments. In the two simulations, the hydraulic conductivities for groundwater and river interaction are not equal. Because the base flow of sub-catchment 1 (up to gauge D-1) is higher than sub-catchment 2 (up to gauge D-2) (Figure 7 and Figure 8), the conductivity of groundwater used for sub-catchment 1 is higher than sub-catchment 2 in the case of multiple sub-catchments simulation. The value for sub-catchment 3 is considered as same as sub-catchment 2. For the case of using the single whole catchment, the conductivity of groundwater is taken as the average of the multiple sub-catchments.

As seen from above results, the agreement of the simulated hydrograph with the observed one at gauge D-2 (Figure 8) is better than the others. The simulation error at gauge D is mainly from the sub-catchment 1 (gauge D-1) according to the results. This can be seen by comparing the observed discharge data at gauge D by adding the discharges at gauge D1 and gauge D2 (Figure 11). From Figure 11, it is found that the observed discharge at gauge D is less than the sum of the observed discharges at gauges D-1 and D-2 in all of the peaks. That means there may be some error in the observed discharge data at D1, most likely in the high flow component.

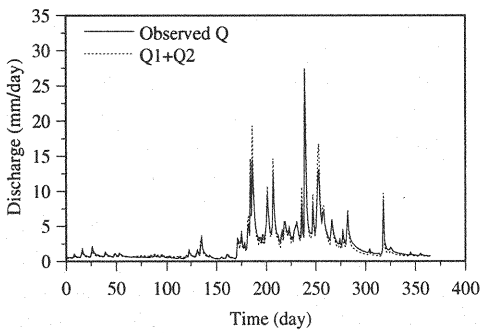

Figure 11 Check of Observed Discharge at Gauge D in 1993

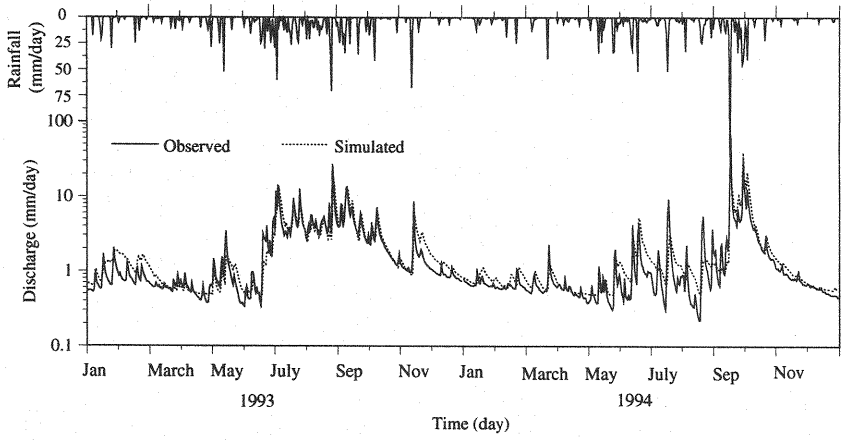

Figure 12 Hydrograph at D for the Case of Single Whole Catchment and Flow Interval Length Less than 600m in 1993 and 1994

It is also necessary to examine the model performance in different year. The weather was wet all over Japan in 1993, but it was dry in 1994. The average rainfall of the Karasu River basin was 1560 mm in 1993 and 1368 mm in 1994. Figure 12 shows the simulation results at gauge D for the Case of Single Whole Catchment and Flow Interval Length Less than 600m in 1993 and 1994. It was found that the agreement of the simulated hydrograph with the observed one is generally good. The simulation error for 1994 is little higher than 1993.

CONCLUSIONS

As can be seen from the results shown above, the methodology gives good results for both the whole catchment and sub-catchments. It indicates that the geomorphologic area function provides an effective means for representing the catchment spatial heterogeneity. For the Karasu River, two years hydrological simulation results in both cases of single whole catchment and three sub-catchments are very close. The flow interval length does not have much impact on hydrological simulation results. The size of sub-catchment used in the geomorphology-based hydrological model can be 1000 km^2, and the flow interval length of two times of DEM resolution is fine enough for hydrological simulation.

The computation time spent for the two-year hydrological simulation with hourly time resolution in 1000 km^2 catchment by Dec-Alpha 433 MHz computer is about 30 seconds. Due to the fast computation advantage, this model can be applied to large river basins. In the present study we used only the spatial distributions of hillslope length, the slope angle and the rainfall. The methodology can be extended to treat land cover, soil type and other parameter variations depending on the availability of data and the simulation needs.

REFERENCE

1. Yang, D., S. Herath and K. Musiake: Analysis of geomorphologic properties extracted from DEMs for hydrologic modeling, Annual Journal of Hydraulic Engineering, Vol.41, pp105-110, 1997a.
2. Naden P. S.: Spatial variability in flood estimation for large catchments: the exploitation of channel network structure, Hydrological Sciences Journal, 37(1), pp53-71, 1992.
3. Yang, D., S. Herath and K. Musiake: Simulation of catchment rainfall-runoff using area function and tank model, Proc. Annu. Conf. JSCE, 52(II), pp324-325, 1997b.
4. Yang, D., S. Herath, K. Musiake. and T. Nakaegawa: Development of a simplified physically-based hillslope response model for modeling flood in mountainous catchments, Proc. Annu. Conf. Japan Soc. Hydrol. and Water Resour, pp57-58, 1997c.

(Received October 5, 1998 ; revised June 1, 1999)